

Safety Metrics and Losses for Object Detection in Autonomous Driving*

Hsuan-Cheng Liao^{†‡}, Chih-Hong Cheng[§], Hasan Esen[†], Alois Knoll[‡]

Abstract—State-of-the-art object detectors have been shown effective in many applications. Usually, their performance is evaluated based on accuracy metrics such as mean Average Precision. In this paper, we consider a safety property of 3D object detectors in the context of Autonomous Driving (AD). In particular, we propose an essential safety requirement for object detectors in AD and formulate it into a specification. During the formulation, we find that abstracting 3D objects with projected 2D bounding boxes on the image and bird’s-eye-view planes allows for a necessary and sufficient condition to the proposed safety requirement. We then leverage the analysis and derive qualitative and quantitative safety metrics based on the Intersection-over-Ground-Truth measure and a distance ratio between predictions and ground truths. Finally, for continual improvement, we formulate safety losses that can be used to optimize object detectors towards higher safety scores. Our experiments with public models on the MMDetection3D library and the nuScenes datasets demonstrate the validity of our consideration and proposals.

I. INTRODUCTION

Object detection has been extensively studied and seen in many applications, such as production line automation and automatic checkouts. It refers to simultaneously classifying and localizing potentially many objects within a single-frame input. Similar to other applications, Autonomous Vehicles (AVs) also depend heavily on object detection models. Indeed, an AV needs the capability to detect objects in its surroundings to avoid collisions and drive safely. Still, one significant difference between AVs and other applications is the safety-criticality in nature. It might be acceptable to misdetect an apple on a counter, but it certainly is not for an AV to misdetect a pedestrian.

Regarding safety in Autonomous Driving (AD), many studies have tackled challenges from various aspects, such as robust model design, effective testing methods, or complete runtime monitors. However, most of the work base their findings on generic metrics such as mean Average Precision (mAP), which in turn uses the Intersection-over-Union (IoU) measure for object detection tasks [1]. We doubt if these metrics fundamentally reflect safety in the context of AD.

[†]Hsuan-Cheng Liao and Hasan Esen are with DENSO AUTOMOTIVE Deutschland GmbH, 85386 Eching, Germany. h.liao, h.esen@eu.denso.com

[§]Chih-Hong Cheng is with Fraunhofer Institute for Cognitive Systems IKS, 80686 Munich, Germany. chih-hong.cheng@iks.fraunhofer.de

[‡]Hsuan-Cheng Liao and Alois Knoll are with Department of Informatics, Technical University of Munich, 85748 Garching, Germany. knoll@in.tum.de

* This project has received funding from the European Union’s Horizon 2020 research and innovation programme under grant agreement No 956123 - FOCETA.

This motivates us to investigate what outputs produced by an object detector can be considered safe and what cannot. Such a practice has also been advocated in industrial safety standards such as ISO 21448 [2] and UL 4600 [3]. Our work can serve as an instantiation of the processes and considerations specified in the safety standards.

Generally, for an object detector, the input can be a 2D camera image or 3D LiDAR point cloud at a time step. The output should be a set of detected objects with their class labels and 3D attributes such as position, dimension, and orientation. We begin our argumentation by naming a safety requirement for such an object detection task in AD: From the perspective of collision avoidance, the object detector is required to cover all objects with predictions, and the predicted distances should not be farther than the ground-truth object distances. Based on this requirement, we derive a specification using projected 2D perspective-view (PV) and bird’s-eye-view (BEV) bounding boxes (BBs). We find that combining these two views enables the formulation of a necessary and sufficient condition to the requirement. Subsequently, we synthesize qualitative and quantitative safety metrics from the specification. We find Intersection-over-Ground-Truth (IoG) a better measure than IoU in modelling safety as per our definition. Lastly, we propose safety losses for optimizing neural networks (NNs) towards safety-by-design performance. We conduct small-scale experiments with the MMDetection3D library [4] and nuScenes dataset [5]. The results demonstrate that the safety metrics deviate from the generic metrics and reflect safety better. Likewise, the safety losses tune object detectors towards higher safety scores while maintaining their performance in the generic metrics. In summary, our contributions include:

- A fundamental safety requirement for 3D object detectors in AD and its necessary and sufficient specification;
- Qualitative and quantitative safety metrics for practical safety evaluation of object detectors;
- Safety losses for optimizing models towards safety-by-design performance; and
- Empirical studies showcasing the validity of our proposals.

The remainder of the paper is organized as follows: Section II highlights some related work, focusing first on generic metrics and losses for object detection and then on safety metrics in AD. Then, Section III introduces more details of the object detection task. Subsequently, Section IV articulates the safety requirement and formulates a specification based on it. Section V and Section VI further synthesizes the

safety metrics and losses for evaluation and optimization, respectively. Section VII presents the experimental setting and results, and finally, Section VIII gives the summary of our work and outlook for future directions.

II. RELATED WORK

This section presents the related work on generic metrics and losses for object detection as well as safety assurance studies in AD.

A. Object Detection Metrics and Losses

We briefly describe generic metrics and losses to motivate our research in the following. For more details, we defer readers to a recent survey paper [1].

The most widely accepted evaluation metric for object detection is mean Average Precision (mAP). However, the calculation process of mAP depends on many parameters, including the estimated confidence levels of the predictions, a predefined IoU threshold, and the Precision-Recall curve interpolation method [1]. To illustrate, another recent work [6] lists a total number of 14 variants of the above process. We observe two issues in such circumstances. First, reported results in existing studies might not be as sound as they seem. Evaluation parameters could be tuned in favor of better numeric scores. Second, it is not straightforward to see the connection between these accuracy metrics and safety properties. Therefore, in this work, we propose a sound and practical process for safety evaluation of 3D object detectors, i.e., *if given a full safety score, an object detector is guaranteed to have performed safely according to our safety requirement.*

We now review losses (or loss functions), an indispensable ingredient to guide data-driven models towards better performance. Generally, a loss function for an object detector can be separated into a classification and a localization element. For classification, the community has shifted from conventional losses such as Cross-Entropy Loss to Focal Loss [7] and its variants to prioritize hard negatives in an object detection paradigm. For localization, there have been two major branches. The first branch uses norm-based losses (e.g., L_1 , Smooth- L_1 , or L_2 norm) to independently penalize errors of BB parameters, including center or corner coordinates and dimensions. Although such formulations help disentangle the complex localization subtask, another branch of studies has found them not necessarily reflective of the localization correctness [8], [9]. Hence, loss functions directly engaging the IoU measure or its variants have been developed to improve the performance, possibly at the expense of slower convergences. More recently, some studies have proposed loss functions in between, showing fast and accurate convergences [10], [11]. Their formulations usually contain a IoU-based term and combine norm-based terms on BB parameters. Inspired by their work, we also attempt to formulate safety losses that can optimize object detectors for higher safety scores.

B. Safety Assurance for AD

As AVs advance rapidly with modern algorithms such as NNs, safety assurance for these systems have gathered more research focuses. An overview of recent studies can be found in [12].

To highlight a few, there are system-level studies evaluating AVs with safety indicators such as mean time/distance between crashes/disengagements [13]. While these measurements generally give a good overview on the performance of the AVs, they do not provide deep insights into the component performance. For this, there have been methods and tools such as probabilistic model checking or testing frameworks for NNs [14]. We introduce several works dedicated to safety in the following and defer interested readers in general verification and validation (e.g., coverage-driven testing) to the survey paper [15]. One major difference between safety-oriented researches and other testing works is that the notion of safety is often task-specific. For example, in [16], the authors inspect practical considerations such as label ambiguity and misclassification tolerances for assessing safety of 2D semantic segmentation models. Likewise, there have been studies integrating safety notions such as response time (based on the Responsibility-Sensitive Safety model [17]) into object detection and tracking metrics [18]. Lastly, for compensating potential insufficiency of NN models, some works introduces post-processing steps to correct the outputs of the models [19], [20], [21]. The results showcase a data-driven method [19], [20] and an analytical formulation [21], based on the IoU measure, for expanding 2D predicted BBs and ensuring full enclosure of ground truths.

Our work complements the aforementioned works in two ways. First, while most works focus on the IoU measure, we find IoG particularly relevant to safety for object detectors. Second, apart from evaluation metrics and post-processing, we further compose safety losses for optimizing the models.

III. FOUNDATION

As introduced, an object detection task involves classifying and localizing objects in a single-frame input. Regardless of the input type, a camera image or lidar point cloud, an object detector predicts a set of detected objects encoded by their attributes, such as object class labels and locations. We denote the predictions as $\mathbf{PD} = \{\mathbf{PD}^i = [\text{PD}^i c^i, \text{PD}^i \ell^i] \mid i \in \mathbb{N}_M\}^1$, where M is the number of detected objects, $\text{PD}^i c^i \in \mathbb{N}_C$ is the class label and $\text{PD}^i \ell^i \in \mathbb{R}^L$ contains the location, dimensions and orientation of the i -th object. The common practice abstracts objects with upright 3D BBs placed horizontally on the ground, as shown in Fig. 1 [1]. It follows that $\ell := {}_{3D}\mathbf{B} = [x_c, y_c, z_c, h, w, l, r] \in \mathbb{R}^7$, where $[x_c, y_c, z_c] = \mathbf{c} \in \mathbb{R}^3$ denotes the center of the BB, $[h, w, l] \in \mathbb{R}^3$ the BB dimensions, and $r \in \mathbb{R}$ the rotational angle around the gravitational direction (omitting the superscripts for prediction PD, ground truth GT, and the object index i).

For evaluation, there shall be a corresponding set of ground truths usually provided by human annotators, denoted

¹Let $M \in \mathbb{N}$, $\mathbb{N}_M := \{x \mid 1 \leq x \leq M, x \in \mathbb{N}\}$ in our work.

as $\widetilde{\mathbf{GT}} = \{\mathbf{GT}^i = [\mathbf{GT}^i c^i, \mathbf{GT}^i \ell^i] \mid i \in \mathbb{N}_N\}$. M could be different from N due to functional insufficiencies of the object detector or arguably human annotation ambiguities [16]. Post-processing, such as non-maximum suppression (NMS) or bipartite matching, is then employed to help relate the two sets of predicted and ground-truth objects. In the following sections, we assume ground truths are perfect without noises such as sensor failures or labeling errors, and M is equal to N . We also assume the AV is modeled as a point at the origin $\mathbf{o} := (0, 0, 0) \in \mathbb{R}^3$.

IV. THE SAFETY REQUIREMENT AND SPECIFICATION

We state our safety requirement and formalize it into a specification in this section.

A. The Safety Requirement

In Section II-A, we have seen several generic metrics for evaluating the accuracy of object detector outputs against ground truths. Our work, on the contrary, aims at constructing a metric that evaluates the safety of object detector outputs, particularly in the context of AD. To such end, we propose a fundamental, if not the only, safety requirement for the object detector:

Requirement 1. *Given an input, the object detector shall localize the objects such that the predictions cover their ground truths from the AV's perspective and that the predictions are estimated not farther than the ground truths.*

The idea is depicted in Fig. 1. If Requirement 1 is fulfilled, then the object detector is said to be safe. The rationale is that as long as the object detector does not overestimate the object distances and covers the ground truths with predictions, the motion planner shall react at least as safely as if the objects are detected at the ground-truth distances². Notably, Requirement 1 only handles what we called safety. As one may observe, the object detector will be evaluated safe if it simply places all predictions just in front of the AV, but it is not functionally effective in this way. One would still rely on the aforementioned generic metrics for distinguishing such cases. Our proposal does not replace the generic metrics but complements them with a notion of safety (as defined in Requirement 1). Likewise, we do not require correct classification. From a safety perspective, we argue that the AV should avoid colliding with any class of objects, and no object should be weighted more importantly than others. Nevertheless, class weighting mechanisms that reflect more granular decision making [22] can still be

²In an AD pipeline, there is usually an object tracker and trajectory predictor in between the object detector and the motion planner. Concerning the two functional components' safety will introduce certain advantages and challenges. For example, an object could be misdetected in one of several consecutive frames as long as the object tracker is still aware of its existence. On the other hand, the relative velocity between the AV and the object has to be considered. Even if the object is estimated at a shorter distance by the object detector at time t and $t+1$, an inaccurate motion model calculated by the object tracker and the trajectory predictor might lead to unsafe path planning and, thus, a collision at time $t+2$. Nonetheless, these concerns are out-of-scope in our work, and we focus on single-frame outputs for object detection.

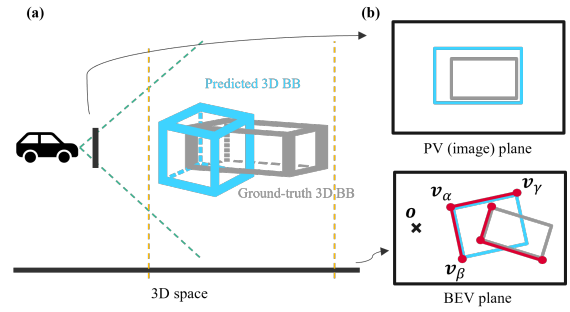


Fig. 1: 3D object abstractions via (a) 3D bounding boxes (BBs) and (b) 2D perspective-view (PV) and bird's-eye-view (BEV) BBs, which Requirement 1 and Specification 2 employs. For simplicity, the actual object is not depicted but assumed to be contained in the ground-truth BB. The predictions are colored in blue and ground truths in grey. Additionally, on the BEV plane, the ego vehicle is marked by the black cross, and the BBs' close-to-AV vertices and frontal sides are highlighted in red.

integrated. For now, we focus on our safety requirement (i.e., Requirement 1) and formalize it in the following.

B. Formalizing Requirement into Technical Specification

For formalizing Requirement 1, we propose to use PV and BEV abstractions of the 3D BBs as shown in Fig. 1. Indeed, if one can ensure the predicted 3D BBs contain the ground-truth 3D BBs, Requirement 1 will be satisfied. However, we argue that this is not necessary. This is because during driving, one only cares about the frontal sides of the obstacles but not the back sides. A predicted 3D BB can actually be smaller than (and hence not containing) the ground-truth 3D BB but still covers it from the AV's perspective. Therefore, to precisely formalize Requirement 1, we consider projecting the 3D BBs onto the PV and BEV planes.

We first address the PV projection. Essentially, during PV projection, a 3D BB is linearly projected onto an image plane using a center of projection (e.g., the origin) and an axis-aligned 2D BB will be placed over the projection. This results in a 2D PV BB defined as ${}_{\text{PV}}\mathbf{B} = [{}_{\text{PV}}x_c, {}_{\text{PV}}y_c, {}_{\text{PV}}h, {}_{\text{PV}}w] \in \mathbb{R}^4$, where $[{}_{\text{PV}}x_c, {}_{\text{PV}}y_c] \in \mathbb{R}^2$ denotes the center, and ${}_{\text{PV}}h \in \mathbb{R}$ and ${}_{\text{PV}}w \in \mathbb{R}$ the height and width. To ensure all predictions cover their ground truths, as stated in the first clause of Requirement 1, we define:

$${}_{\text{PV}}\Pi := \forall i \in \mathbb{N}_N : {}_{\text{PV}}^{\text{GT}}\mathbf{B}^i \subset {}_{\text{PV}}^{\text{PD}}\mathbf{B}^i, \quad (1)$$

where $\mathbf{P} \subset \mathbf{Q}$ denotes that BB \mathbf{P} is contained in BB \mathbf{Q} . In practice, this can be quickly checked with image coordinates of the 2D PV BB vertices.

Next, we project 3D BBs to 2D BEV BBs. This is done by outlining the smallest oriented 2D BB around the projected polygon of the 3D BB on the BEV plane (as shown in Fig. 2). Mathematically, this leads to ${}_{\text{BEV}}\mathbf{B} = [{}_{\text{BEV}}x_c, {}_{\text{BEV}}y_c, {}_{\text{BEV}}l, {}_{\text{BEV}}w, {}_{\text{BEV}}r] \in \mathbb{R}^5$, where $[{}_{\text{BEV}}x_c, {}_{\text{BEV}}y_c] \in \mathbb{R}^2$ is the center, ${}_{\text{BEV}}l \in \mathbb{R}$, ${}_{\text{BEV}}w \in \mathbb{R}$ and ${}_{\text{BEV}}r \in \mathbb{R}$ the length, width and the rotational angle around the gravitational direction. Now, based on (1), we consider adding two conditions for fully formalizing Requirement 1. First, the closest vertex of the predicted BEV BB has to be closer than the ground truth's. Second, the two frontal sides of the predicted BEV

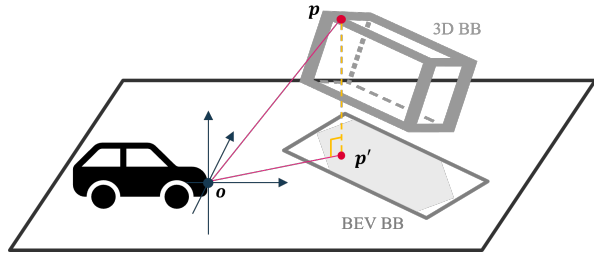


Fig. 2: Orthographic projection of a 3D ground-truth BB to a BEV 2D BB, where the 3D BB is possibly tilted due to undulating roads.

BB do not intersect with the ground-truth ones³. Altogether, we formalize Requirement 1 as:

$$\begin{aligned}
\Pi &=_{\text{PV}} \Pi \wedge \overset{\text{dist}}{\text{BEV}} \Pi \wedge \overset{\not\perp}{\text{BEV}} \Pi \\
&:= \forall i \in \mathbb{N}_N : \overset{\text{GT}}{\text{PV}} \mathbf{B}^i \subset \overset{\text{PD}}{\text{PV}} \mathbf{B}^i \wedge \text{dist}(\overset{\text{PD}}{\text{BEV}} \mathbf{v}_\alpha^i) \leq \text{dist}(\overset{\text{GT}}{\text{BEV}} \mathbf{v}_\alpha^i) \\
&\wedge \overset{\text{PD}}{\text{BEV}} \mathbf{v}_\alpha^i \overset{\text{PD}}{\text{BEV}} \mathbf{v}_\beta^i \not\perp \overset{\text{GT}}{\text{BEV}} \mathbf{v}_\alpha^i \overset{\text{GT}}{\text{BEV}} \mathbf{v}_\beta^i \wedge \overset{\text{PD}}{\text{BEV}} \mathbf{v}_\alpha^i \overset{\text{PD}}{\text{BEV}} \mathbf{v}_\gamma^i \not\perp \overset{\text{GT}}{\text{BEV}} \mathbf{v}_\alpha^i \overset{\text{GT}}{\text{BEV}} \mathbf{v}_\gamma^i \\
&\wedge \overset{\text{PD}}{\text{BEV}} \mathbf{v}_\alpha^i \overset{\text{PD}}{\text{BEV}} \mathbf{v}_\gamma^i \not\perp \overset{\text{GT}}{\text{BEV}} \mathbf{v}_\alpha^i \overset{\text{GT}}{\text{BEV}} \mathbf{v}_\beta^i \wedge \overset{\text{PD}}{\text{BEV}} \mathbf{v}_\alpha^i \overset{\text{PD}}{\text{BEV}} \mathbf{v}_\beta^i \not\perp \overset{\text{GT}}{\text{BEV}} \mathbf{v}_\alpha^i \overset{\text{GT}}{\text{BEV}} \mathbf{v}_\gamma^i,
\end{aligned} \tag{2}$$

where $\overline{\mathbf{ab}} \not\perp \overline{\mathbf{cd}}$ denotes that the two line segments do not intersect, and $\mathbf{v}_{\alpha/\beta/\gamma}$ are the close-to-AV vertices as highlighted in Fig. 1b.

As such, we ensure that the predictions cover the ground truths and are estimated not farther than them. We state two remarks at this point to further justify our usage of PV and BEV BBs. First, it is necessary to have the BEV conditions (i.e., $\overset{\text{dist}}{\text{BEV}} \Pi \wedge \overset{\not\perp}{\text{BEV}} \Pi$) for satisfying Requirement 1. The fact that a predicted 2D PV BB contains its ground-truth counterpart (i.e., $\overset{\text{PV}}{\Pi}$) does not imply that the 3D prediction is made in front of the 3D ground truth from the AV. A counterexample is as follows: The predicted 3D BB could be farther yet much larger than the ground-truth 3D BB such that after a perspective projection, the predicted 2D PV BB still covers its ground-truth counterpart. Therefore, one needs the 2D BEV conditions.

The second remark is that having the 2D PV condition (i.e., $\overset{\text{PV}}{\Pi}$) increases the precision of modelling Requirement 1 into a specification. Similar to the case of 3D BB abstraction, 2D BEV BB abstraction can soundly satisfy Requirement 1 by its own. For instance, one can specify that predicted 2D BEV BBs shall fully contain ground-truth 2D BEV BBs⁴. However, this is also not necessary. With the 2D PV condition, one only has to specify the additional two 2D BEV conditions regarding the closest vertex and the frontal sides. Thus, our formalized Specification Π gives the necessary and sufficient conditions to Requirement 1.

³We note a special case where a BEV BB is perpendicularly facing the AV. In this case, our specification considers the front-facing side and either of the adjacent sides of the BEV BB

⁴The soundness of this BEV specification is attributed to the geometric property of orthographic projection. Specifically, as shown in Fig. 2, it always holds that $\overline{\mathbf{op}} \geq \overline{\mathbf{op}'}$. Additionally, the BEV BB always contains the projected polygon, hence the soundness.

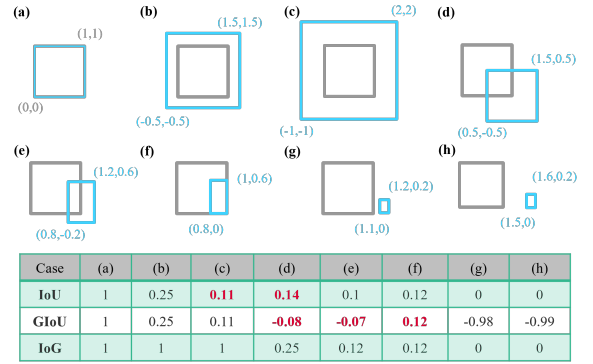


Fig. 3: A comparison of IoU, GloU, and IoG. The ground truth BB (in grey) is always spanning from (0,0) to (1,1), and the prediction (in blue) varies over cases. The values in red highlight the cases where the metric fails to model our safety notion.

V. SAFETY METRICS FOR MODEL EVALUATION

We now leverage the analysis in the previous section and synthesize a qualitative and a quantitative safety metric for evaluating object detectors.

A. Qualitative Safety Metric

A qualitative safety metric can be formulated straightforwardly. To illustrate, it is responsible for evaluating whether a set of outputs of an object detector, when compared against the set of corresponding ground truth, is safe or not. With the specification in (2), we can formulate it as follows:

$$S_{q1}(\widetilde{\mathbf{PD}}, \widetilde{\mathbf{GT}}) := \Pi ? 1 : 0. \tag{3}$$

B. Quantitative Safety Metric

We turn our focus on formulating a quantitative safety metric, which should take a similar responsibility to the qualitative one yet on a finer scale. More specifically, when the object detector performs safely (i.e., fulfilling Specification (2)), it is given a full score (e.g., at 1). On the other hand, when it does not, it is given a numeric value reflecting how unsafe the prediction is (e.g., from 1 to 0)⁵.

We first consider the 2D PV term in (2). Based on our safety specification, the more a predicted BB covers the ground-truth BB, the higher score it should generate. We notice, however, that the commonly used Intersection-over-Union (IoU) measure or its variants (e.g., Generalized-IoU (GIoU) [9]) do not reflect this property well. Instead, it is better modeled by Intersection-over-Ground-Truth (IoG), defined in (4). Fig. 3 depicts different cases for comparing the measures. As a result, we utilize IoG and define the PV-plane score as follows:

$$\begin{aligned}
\text{PV} S_{qn}(\widetilde{\mathbf{PD}}, \widetilde{\mathbf{GT}}) &:= \frac{1}{N} \sum_{i=1}^N \text{IoG}(\overset{\text{PD}}{\text{PV}} \mathbf{B}^i, \overset{\text{GT}}{\text{PV}} \mathbf{B}^i) \\
&= \frac{1}{N} \sum_{i=1}^N \frac{\text{area}(\overset{\text{PD}}{\text{PV}} \mathbf{B}^i \cap \overset{\text{GT}}{\text{PV}} \mathbf{B}^i)}{\text{area}(\overset{\text{GT}}{\text{PV}} \mathbf{B}^i)}.
\end{aligned} \tag{4}$$

⁵As discussed in Section IV-A, among safe predictions, there is no notion of “safer”. They are equally safe, though perhaps unequally accurate.

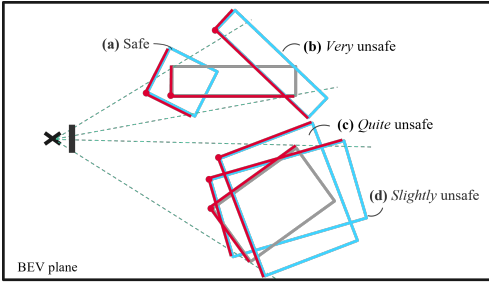


Fig. 4: Different cases of safety evaluation on the BEV plane (all fulfilling the PV-space specification, though). The predictions are in blue, the ground truths in grey, and the closest vertices and frontal sides in red.

Next, we consider the 2D BEV conditions. As shown in Fig. 4, the BEV-plane score should reflect the following cases differently: (a) If the closest vertex of the prediction $\mathbf{v}_{\alpha}^{\text{PD}}$ is closer than that of the ground truth $\mathbf{v}_{\alpha}^{\text{GT}}$ and the frontal sides don't intersect, then the particular prediction is said safe and given a full score (e.g., 1); (b) If $\mathbf{v}_{\alpha}^{\text{PD}}$ is farther than $\mathbf{v}_{\alpha}^{\text{GT}}$, then safety is quantified with the distance ratio and \log between the prediction and the ground truth; (c/d) If $\mathbf{v}_{\alpha}^{\text{PD}}$ is closer than $\mathbf{v}_{\alpha}^{\text{GT}}$ but the frontal sides intersect, then safety is quantified by the \log measure⁶. Now, we mathematically summarize the cases as follows:

$$\begin{aligned} & S_{\text{qn}}^{\text{BEV}}(\widetilde{\text{PD}}, \widetilde{\text{GT}}) \\ & := \frac{1}{2N} \sum_{i=1}^N \left[\min\left(1, \frac{\text{dist}(\mathbf{v}_{\alpha}^{\text{GT}})}{\text{dist}(\mathbf{v}_{\alpha}^{\text{PD}})}\right) + \log\left(\frac{\text{vol}(\mathbf{B}^i_{\text{BEV}}^{\text{PD}})}{\text{vol}(\mathbf{B}^i_{\text{BEV}}^{\text{GT}})}\right) \right] \end{aligned} \quad (5)$$

To summarize, we combine the above PV and BEV terms into two quantitative safety metrics. The first one is based on averaging as follows:

$$S_{\text{qn}}^{\text{sum}}(\widetilde{\text{PD}}, \widetilde{\text{GT}}) := \frac{1}{2} (S_{\text{qn}}^{\text{PV}} + S_{\text{qn}}^{\text{BEV}}). \quad (6)$$

On the contrary, the second one is based on multiplication as follows:

$$\begin{aligned} & S_{\text{qn}}^{\text{pdt}}(\widetilde{\text{PD}}, \widetilde{\text{GT}}) := \frac{1}{N} \sum_{i=1}^N \left\{ \log\left(\frac{\text{vol}(\mathbf{B}^i_{\text{PV}}^{\text{PD}})}{\text{vol}(\mathbf{B}^i_{\text{PV}}^{\text{GT}})}\right) \right. \\ & \quad \left. \times \frac{1}{2} \left[\min\left(1, \frac{\text{dist}(\mathbf{v}_{\alpha}^{\text{GT}})}{\text{dist}(\mathbf{v}_{\alpha}^{\text{PD}})}\right) + \log\left(\frac{\text{vol}(\mathbf{B}^i_{\text{BEV}}^{\text{PD}})}{\text{vol}(\mathbf{B}^i_{\text{BEV}}^{\text{GT}})}\right) \right] \right\}. \end{aligned} \quad (7)$$

VI. SAFETY LOSSES FOR MODEL OPTIMIZATION

In this section, we further formulate safety losses for optimizing 3D object detectors. As discussed in Section II-A, there have been multiple proposals in the literature aligning the optimization losses with the evaluation metrics, eventually generating stronger performances [8], [9], [10], [11]. Likewise, we construct our safety losses based on the safety metrics, in which the \log measure plays a central role. Hence, we define a safety loss component $L_{\log} = 1 - \log\left(\frac{\text{vol}(\mathbf{B}_{3\text{D}}^{\text{PD}})}{\text{vol}(\mathbf{B}_{3\text{D}}^{\text{GT}})}\right)$, where $\log(\cdot, \cdot)$ now takes 3D BB inputs and computes the ratio using volumes of the BBs. This is due to the consideration that the task is performed directly

⁶We note that during quantitative evaluation using the BEV conditions, we fall back to requiring ground-truth BEV BBs to be fully enclosed for lower computation complexity.

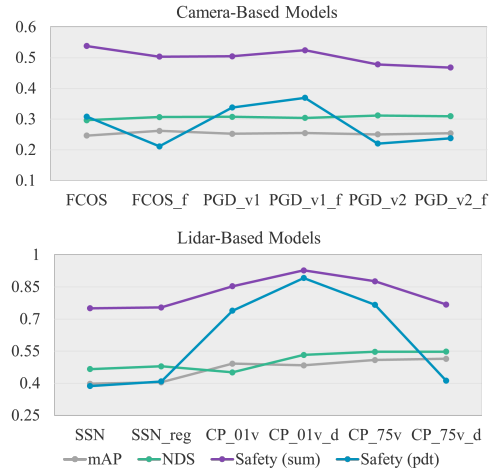


Fig. 5: Evaluation results of different object detectors (trained and provided by [4]) using mean Average Precision (mAP), nuScenes Detection Score (NDS), and our safety metrics.

in the 3D space and the availability of computing algorithms such as Pytorch3D [23]. 2D cases follow similarly.

Nevertheless, as seen in Fig. 3, the safety loss component on its own does not suffice for optimizing an object detector as \log saturates when the prediction reaches a “safe” state. Hence, we combine the safety loss component with the state-of-the-art loss functions for accurate object detection (L_{Acc}), e.g., the SmoothL1 Loss (L_{SmoothL1}) [24] or the Efficient-IoU Loss (L_{EIoU}) [11]. Altogether, we have:

$$\begin{aligned} & \mathcal{L}_{\text{Safe-Acc}}(\mathbf{B}_{3\text{D}}^{\text{PD}}, \mathbf{B}_{3\text{D}}^{\text{GT}}) \\ & = \lambda L_{\log}(\mathbf{B}_{3\text{D}}^{\text{PD}}, \mathbf{B}_{3\text{D}}^{\text{GT}}) + (1 - \lambda) L_{\text{Acc}}(\mathbf{B}_{3\text{D}}^{\text{PD}}, \mathbf{B}_{3\text{D}}^{\text{GT}}), \end{aligned} \quad (8)$$

where $\lambda \in \mathbb{R} : 0 < \lambda \leq 1$ is a balancing hyper-parameter. We note that L_{Acc} can be instantiated by different loss functions depending on the need of the NN architectures, resulting in further safety losses.

VII. EXPERIMENTAL RESULTS AND DISCUSSIONS

We now provide and discuss the experimental settings and results. For experiment, we utilize the public 3D object detection library MMDetection3D [4] and the nuScenes dataset [5]⁷.

A. Evaluating Object Detectors with Safety Metrics

We perform the model evaluation step in a general NN learning pipeline to see our safety metrics’ effectiveness. We select the leading models on the nuScenes dataset, including the camera-based FCOS [25] and PGD [26] as well as the lidar-based CenterPoint [27] and SSN [28]. We also consider their variants generated with different backbones, voxel sizes, or finetuning steps. The relevant details can be found in [4]. We record the evaluation results in Fig. 5 and highlight the following two observations: First, as typically perceived, the lidar-based models are more reliable than camera-based ones, and our safety metrics confirm this. Second, our safety

⁷The utilization of the MMDetection3D library and nuScenes dataset in this paper is for knowledge dissemination and scientific publication, not for commercial use.

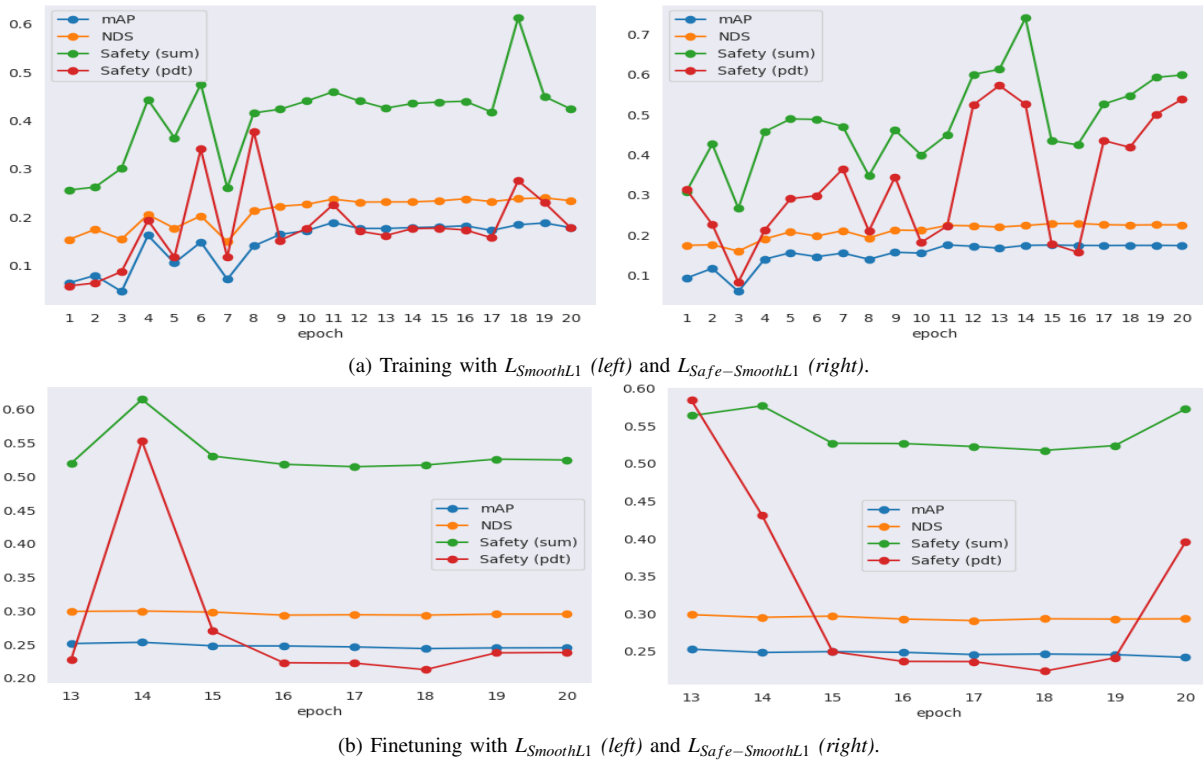


Fig. 6: Optimization results of FCOS3D on nuScenes-mini.

metrics are by themselves consistent and depict different performance profiles from the generic metrics (i.e., mean Average Precision (mAP) and nuScenes Detection Score (NDS) [5]). In particular, our multiplication-based metric (i.e., Safety (pdt)) can significantly differentiate the model performance better than the other metrics. It also shows that more accurate models are not necessarily safer, according to our definition in Requirement (1).

B. Optimizing Object Detectors with Safety Losses

We now close the loop of our work by conducting optimization with an example of the safety losses. Here, we utilize the nuScenes-mini dataset [5] for small-scale experiments and focus on the state-of-the-art monocular 3D object detector FCOS3D [25]. We follow the FCOS3D paper to implement the SmoothL1 loss (i.e., $L_{Acc} = L_{SmoothL1}$) and apply the training settings, such as data augmentation, batch sizes, and learning schemes, as reported in [4].

We first conduct full training from scratch with $L_{SmoothL1}$ and $L_{Safe-SmoothL1}$ (setting $\lambda = 0.2$) for 20 epochs. As seen in Fig. 6a, the model trained with the additional safety loss component achieves higher safety scores (i.e., Safety (sum) and Safety (pdt)) while delivering similar generic scores (i.e., mAP and NDS) compared to the model trained with the SmoothL1 loss only. We also conduct finetuning on trained models. These models are trained with the full nuScenes dataset for 12 epochs by [4]. A similar result can be observed in Fig. 6b. The finetuning process with the safety loss keeps the model’s safety performance better than the other model without degrading the generic metrics. Hence, adding the safety loss component into the general loss formulations is

believed to enhance the safety (as per Requirement (1)) of the object detectors.

VIII. CONCLUSION

This work considers evaluating and improving object detectors in AD concerning safety. We define safety in this context as the detector always predicting objects not farther than their ground truth with full coverage. We then formalize this requirement into a specification by abstracting real-world 3D objects with 2D PV BBs and BEV BBs. Based on this specification, we derive two safety metrics for the actual evaluation. In addition, we propose safety losses for model optimization. Our proposals are shown to be practical and valid with the experiments. The safety metrics depict different performance profiles from those given by generic metrics such as mAP, and our safety loss promotes the detectors’ safety performance while maintaining their generic scores.

Still, there are certain limitations in this work. For example, we consider only single-step input-output relations, whereas real-world systems involve time and motions. One natural extension is to investigate safety requirements for object tracking and trajectory prediction components. Likewise, future studies can identify more safety properties of object detectors. Additionally, larger-scale experiments are required to see the applicability of our proposals to other models, including the lidar-based ones. Finally, the safety losses can be further improved. For instance, using class or distance weighting and better merging safety and accuracy losses beyond using a coefficient are open directions.

REFERENCES

- [1] X. Ma, W. Ouyang, A. Simonelli, and E. Ricci, “3D object detection from images for autonomous driving: a survey,” *arXiv preprint arXiv:2202.02980*, 2022.
- [2] “Road vehicles — safety of the intended functionality,” ISO, Standard ISO 21448, 2022.
- [3] “Evaluation of autonomous products,” UL Standards & Engagement, Standard UL 4600, 2022.
- [4] M. Contributors, “MMDetection3D: OpenMMLab next-generation platform for general 3D object detection,” <https://github.com/open-mmlab/mmdetection3d>, 2020.
- [5] H. Caesar, V. Bankiti, A. H. Lang, S. Vora, V. E. Liong, Q. Xu, A. Krishnan, Y. Pan, G. Baldan, and O. Beijbom, “nusscenes: A multimodal dataset for autonomous driving,” *arXiv preprint arXiv:1903.11027*, 2019.
- [6] R. Padilla, W. L. Passos, T. L. B. Dias, S. L. Netto, and E. A. B. da Silva, “A comparative analysis of object detection metrics with a companion open-source toolkit,” *Electronics*, 2021.
- [7] T.-Y. Lin, P. Goyal, R. Girshick, K. He, and P. Dollár, “Focal loss for dense object detection,” in *ICCV*, 2017.
- [8] J. Yu, Y. Jiang, Z. Wang, Z. Cao, and T. Huang, “Unitbox: An advanced object detection network,” in *ACM Multimedia*, 2016.
- [9] H. Rezatofighi, N. Tsoi, J. Gwak, A. Sadeghian, I. Reid, and S. Savarese, “Generalized IoU,” in *CVPR*, 2019.
- [10] Z. Zheng, P. Wang, W. Liu, J. Li, R. Ye, and D. Ren, “Distance-IoU loss: Faster and better learning for bounding box regression,” in *AAAI*, 2020.
- [11] Y.-F. Zhang, W. Ren, Z. Zhang, Z. Jia, L. Wang, and T. Tan, “Focal and efficient IoU loss for accurate bounding box regression,” *Neurocomputing*, vol. 506, pp. 146–157, 2022.
- [12] S. Houben, S. Abrecht, M. Akila, A. Bär, F. Brockherde, P. Feifel, T. Fingscheidt, S. S. Gannamaneni, S. E. Ghobadi, A. Hammam, A. Haselhoff, F. Hauser, C. Heinzemann, M. Hoffmann, N. Kapoor, F. Kappel, M. Klingner, J. Kronenberger, F. Küppers, J. Löhdefink, M. Mlynarski, M. Mock, F. Mualla, S. Pavlitskaya, M. Poretschkin, A. Pohl, V. Ravi-Kumar, J. Rosenzweig, M. Rottmann, S. Rüping, T. Sämann, J. D. Schneider, E. Schulz, G. Schwalbe, J. Sicking, T. Srivastava, S. Varghese, M. Weber, S. Wirkert, T. Wirtz, and M. Woehrle, “Inspect, understand, overcome: A survey of practical methods for AI safety,” in *Deep Neural Networks and Data for Automated Driving*. Springer International Publishing, 2022, pp. 3–78.
- [13] J. Guo, U. Kurup, and M. Shah, “Is it safe to drive? An overview of factors, metrics, and datasets for driveability assessment in autonomous driving,” *IEEE Trans. Intell. Transp. Syst.*, 2020.
- [14] M. Kwiatkowska, G. Norman, and D. Parker, “Prism: Probabilistic model checking for performance and reliability analysis,” *SIGMETRICS Perform. Eval. Rev.*, vol. 36, p. 40–45, 2009.
- [15] X. Huang, D. Kroening, W. Ruan, J. Sharp, Y. Sun, E. Thamo, M. Wu, and X. Yi, “A survey of safety and trustworthiness of deep neural networks: Verification, testing, adversarial attack and defence, and interpretability,” *Computer Science Review*, vol. 37, p. 100270, 2020.
- [16] C.-H. Cheng, A. Knoll, and H.-C. Liao, “Safety metrics for semantic segmentation in autonomous driving,” in *AITest*, 2021.
- [17] S. Shalev-Shwartz, S. Shammah, and A. Shashua, “On a formal model of safe and scalable self-driving cars,” 2017.
- [18] G. Volk, J. Gamerding, A. v. Bernuth, and O. Bringmann, “A comprehensive safety metric to evaluate perception in autonomous systems,” in *ITSC*, 2020.
- [19] C.-H. Cheng, T. Schuster, and S. Burton, “Logically sound arguments for the effectiveness of ml safety measures,” in *SafeComp Workshops*, 2022.
- [20] F. de Grancey, J.-L. Adam, L. Alecu, S. Gerchinovitz, F. Mamalet, and D. Vigouroux, “Object detection with probabilistic guarantees: A conformal prediction approach,” in *SafeComp Workshops*, 2022.
- [21] T. Schuster, E. Seferis, S. Burton, and C.-H. Cheng, “Unaligned but safe – formally compensating performance limitations for imprecise 2d object detection,” in *SafeComp*, 2022.
- [22] B. Chen, C. Gong, and J. Yang, “Importance-aware semantic segmentation for autonomous vehicles,” *IEEE Transactions on Intelligent Transportation Systems*, 2019.
- [23] N. Ravi, J. Reizenstein, D. Novotny, T. Gordon, W.-Y. Lo, J. Johnson, and G. Gkioxari, “Accelerating 3D deep learning with pytorch3d,” 2020.
- [24] R. Girshick, “Fast R-CNN,” in *ICCV*, 2015.
- [25] T. Wang, X. Zhu, J. Pang, and D. Lin, “FCOS3D: Fully convolutional one-stage monocular 3D object detection,” in *ICCVW*, 2021.
- [26] —, “Probabilistic and Geometric Depth: Detecting objects in perspective,” in *CoRL*, 2021.
- [27] T. Yin, X. Zhou, and P. Krähénbühl, “Center-based 3D object detection and tracking,” in *CVPR*, 2021.
- [28] X. Zhu, Y. Ma, T. Wang, Y. Xu, J. Shi, and D. Lin, “SSN: Shape signature networks for multi-class object detection from point clouds,” in *ECCV*, 2020.